



RESEARCH LETTER

10.1002/2014GL061958

Key Points:

- Azimuthal anisotropy in much of Colombia shows trench-perpendicular fast axes
- Trench-parallel fast axes may be due to a lithospheric signal or slab tear
- Results challenge subduction zone anisotropy and slab dynamics models

Supporting Information:

- Readme
- Table S1 and Figures S1–S3

Correspondence to:

R. W. Porritt,
rporritt@usc.edu

Citation:

Porritt, R. W., T. W. Becker, and G. Monsalve (2014), Seismic anisotropy and slab dynamics from SKS splitting recorded in Colombia, *Geophys. Res. Lett.*, 41, doi:10.1002/2014GL061958.

Received 22 SEP 2014

Accepted 24 NOV 2014

Accepted article online 28 NOV 2014

Seismic anisotropy and slab dynamics from SKS splitting recorded in Colombia

Robert W. Porritt¹, Thorsten W. Becker¹, and Gaspar Monsalve²

¹Department of Earth Sciences, University of Southern California, Los Angeles, California, USA, ²Facultad de Minas, Departamento de Geociencias y Medio Ambiente, Universidad Nacional de Colombia, Medellín, Colombia

Abstract The Nazca, Caribbean, and South America plates meet in northwestern South America where the northern end of the Andean volcanic arc and Wadati-Benioff zone seismicity indicate ongoing subduction. However, the termination of Quaternary volcanism at $\sim 5.5^{\circ}\text{N}$ and eastward offset in seismicity underneath Colombia suggest the presence of complex slab geometry. To help link geometry to dynamics, we analyze SKS splitting for 38 broadband stations of the Colombian national network. Measurements of fast polarization axes in western Colombia close to the trench show dominantly trench-perpendicular orientations. Orientations measured at stations in the back arc, farther to the east, however, abruptly change to roughly trench parallel anisotropy. This may indicate along-arc mantle flow, possibly related to the suggested “Caldas” slab tear, or a lithospheric signature, but smaller-scale variations in anisotropy remain to be explained. Our observations are atypical globally and challenge our understanding of the complexities of subduction zone seismic anisotropy.

1. Introduction

Subduction of multiple plates in northwestern South America is expressed in the offset of Andean topography in Colombia, complex seismicity indicating several slab segments, and the termination of Andean volcanism at $\sim 5.5^{\circ}\text{N}$. This has been explained by a northeastern (“Bucaramanga”) and a southwestern (“Cauca”) slab segment, in the nomenclature of *Pennington* [1981], with the separation coincident with the extent of volcanism [e.g., *Pennington*, 1981; *van der Hilst and Mann*, 1994; *Taboada et al.*, 2000; *Gutscher et al.*, 2000; *Ojeda and Havskov*, 2001; *Cortés and Angelier*, 2005; *Vargas and Mann*, 2013; *Yarce et al.*, 2014]. However, the origin of the different slab segments and their respective subduction angle remains debated. For example, it was recently suggested that the cause of the segmentation may be the “Caldas Tear,” a slab gap inferred to be associated with the southern end of a 12 Ma Caribbean oceanic arc [*Vargas and Mann*, 2013].

There are currently two prevailing hypotheses for the separation of the Cauca and Bucaramanga segments. One suggests that the Cauca segment is the northern termination of the subducting Nazca Plate, while the Bucaramanga segment represents an older piece of the Caribbean Plate that has rotated into its current geometry following closure of the Isthmus of Panama [e.g., *Pennington*, 1981; *Montes et al.*, 2012; *Vargas and Mann*, 2013]. Alternatively, the seismicity patterns may correspond to a folded or torn slab, or two pieces of the Nazca Plate that have been separated by a transform fault and are now subducting independently. This alternative explains the offset and near-parallel strikes but seems difficult to reconcile with the surface plate reorganizations during the closure of the Isthmus of Panama [e.g., *Montes et al.*, 2012].

Interpretation of mantle structure should ideally be reflected in a dynamically consistent model that includes predictions of mantle flow around slabs. Observations of seismic anisotropy lend themselves to put constraints on such models, particularly from measurements of teleseismic (SKS) shear wave splitting [e.g., *Silver*, 1996]. For the upper mantle, we expect that the alignment of intrinsically anisotropic olivine crystals under recent mantle flow, or frozen in from prior convective episodes, is the main cause of anisotropy. The polarization plane of the fast propagating wave (“fast axis”) of shear wave splitting is then expected to align roughly with the shear direction via formation of “A”-type lattice-preferred orientations (LPOs) along the raypath [e.g., *Mainprice*, 2007]. Alternatively, other olivine fabrics such as B or C type may be present under high-stress and -water content conditions [e.g., *Karato et al.*, 2008]. In this case, fast axes would be oriented perpendicular to mantle shearing, but we expect those regions to contribute less to the signal, and, globally, A-type LPO provides a valid model for azimuthal anisotropy underneath oceanic plates [*Becker et al.*, 2014].

Corner flow-type mantle circulation in subduction zones predicts a sense of shear with orientation, and hence fast axes, aligned perpendicular to the trench [e.g., *McKenzie, 1979*]. However, subduction zone anisotropy based on *SKS* splitting often shows trench-parallel alignment, particularly when sensing the subslab mantle [*Long and Silver, 2008*]. This has been attributed to a number of causes, and many of the models for the wedge and subslab region are reviewed in *Long and Becker [2010]*. Explanations include differences in LPO formation, contributions from inherited structure in the slab, or minerals other than olivine, to anisotropy, and more complex, 3-D flow fields around slabs. Those asthenospheric flow models invoke slab dip variations [*Kneller and van Keken, 2008*], slab gaps [e.g., *Eakin et al., 2010*], or realignment of flow caused by relative trench motions [e.g., *Buttles and Olson, 1998; Hall et al., 2000; Druken et al., 2011; Faccenda and Capitanio, 2013; Li et al., 2014*].

Previous observations of anisotropy in South America away from subduction zones show primarily east-west fast axes (Figure 1). Closer to the trench, along the Pacific subduction zones, trench-parallel anisotropy is often, but not always, observed. *Russo and Silver [1994]* interpreted the trench-parallel fast axes as being caused by slab-induced stirring in the mantle, and some version of this model, perhaps in combinations with the effects mentioned above, is often invoked to explain trench-parallel anisotropy. However, the global subduction zone anisotropy signal is complex, and a comprehensive model seems elusive [*Long, 2013*]. Here we set out to complement the South American anisotropy data set by providing additional *SKS* splitting measurements for the tectonically complex and dynamically important region of western Colombia.

2. Shear Wave Splitting Measurements

We performed *SKS* splitting measurements for seismic waveforms as recorded at stations of the National Seismological Network of Colombia (*Red Sismológica Nacional de Colombia, RSNC*). We were able to obtain splitting parameters at 18 out of the 38 stations (Table S1 in the supporting information) for the data set that was available to us (April 2008 to December 2012, though not all stations were operational throughout the entire time period). The stations are distributed throughout western Colombia, primarily along the high topography of the Colombian cordilleras (see Figure S1 for station locations and names). *SKS* splitting parameters were obtained using *SplitLab* [*Wüstefeld et al., 2008*], selecting events larger than magnitude *M*₅ with epicentral distance between 90° and 130°. Velocity-proportional seismograms were windowed around the *SKS* arrival when observed on the radial and vertical channels and band-pass filtered between 0.02 and 0.1 Hz. *SplitLab* estimates the splitting delay time and fast axis by three methods: maximum correlation between fast and slow axes (rotation correlation, RC) [*Bowman and Ando, 1987*], minimum energy on the transverse component (SC) [*Silver and Chan, 1991*], and the eigenvalue method (EV) [*Silver and Chan, 1991*]. For our data set, we find that the RC method has the most consistent results as was also found and discussed by *Miller et al. [2013]*. In order to ensure the highest-quality splitting measurements, we only present “good” results, as defined by visual assessment considering limited trade-off in misfit plots, consistency between the RC and SC methods, a flattened transverse component, and particle motion collapsed from elliptical to linear. Examples of good splitting at stations HEL and BRR are shown in Figure S2, but many of the events recorded were too noisy to allow single-event shear wave splitting measurements. Table 1 lists the mean fast axis and delay time at each station, and Table S1 presents the individual splitting parameters for all three methods. Practical limitations such as interrupted recording and high noise level limit us to present far fewer splits, with reduced back azimuthal coverage, than would be expected based on the global seismicity distribution during the study period.

All of our new splitting parameters are shown in Figure 2. The inferred fast axes of azimuthal anisotropy are oriented east-west in southern Colombia, north-south in the Eastern Cordillera, and rotate from east-west to northwest-southeast in the northern Central Cordillera. These areas also have relatively large delay times between 1 and 2 s. Areas with low topography, such as the Magdalena Valley located between the Eastern and Central Cordillera, and the northwest along the Colombian Caribbean coast show smaller amplitude splitting delay times (<1 s) or lack good observations. Four stations in these low-lying regions had no good quality splitting measurements, while four stations in the Eastern Cordillera and three in the Western Cordillera also lack acceptable observations. No clear null splits were observed in the data set. The

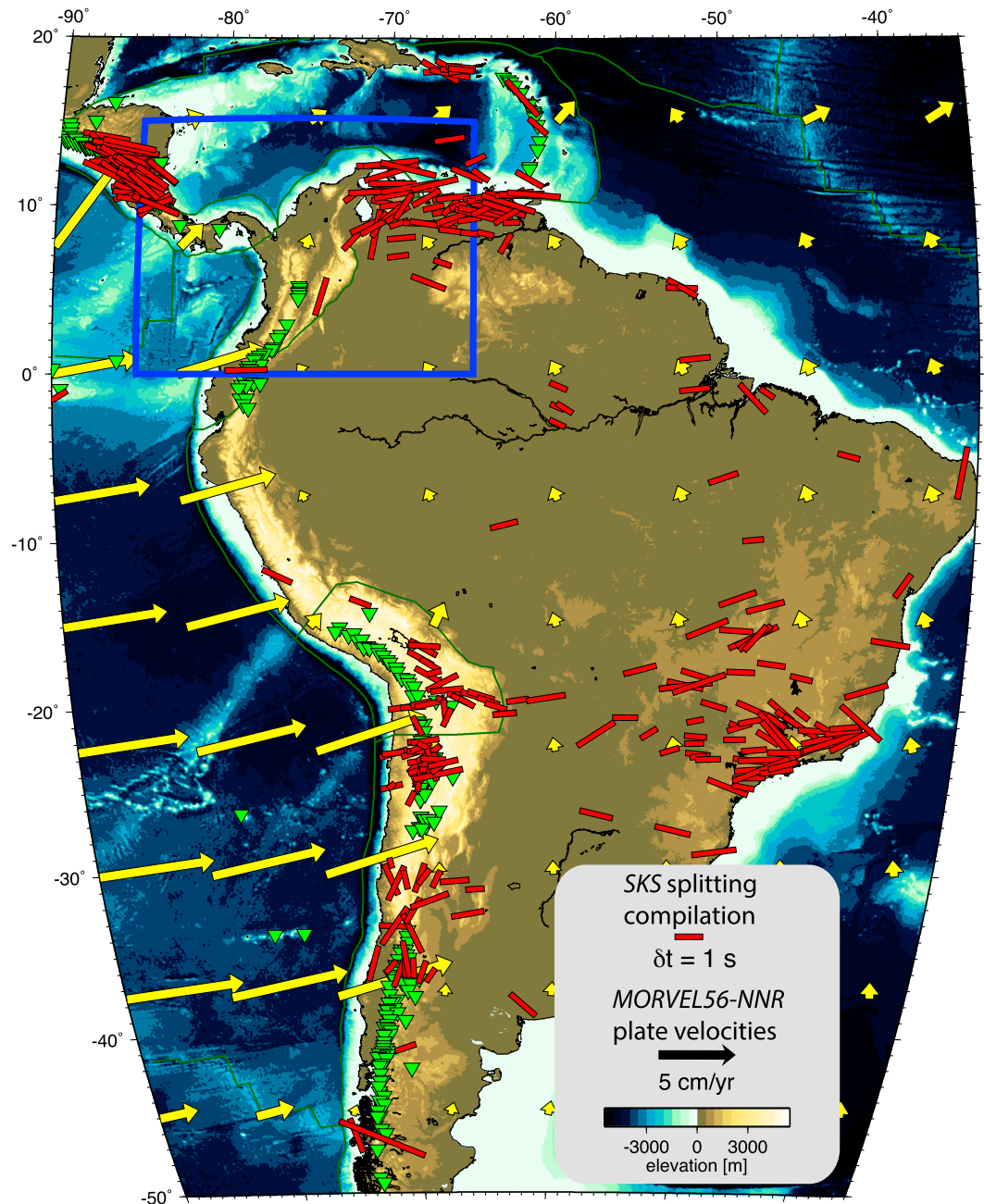


Figure 1. Previous, station-averaged SKS splitting measurements (red sticks), plate velocities in a no-net rotation reference frame (yellow arrows, MORVEL56-NNR [Argus et al., 2011]), and quaternary volcanoes (green inverted triangles, Smithsonian Institute volcanoes program, <http://www.volcano.si.edu/>, accessed 09/2014). Blue rectangle outlines region evaluated in Figures 2 and 3. SKS measurements are from Becker et al. [2012] and updates of the Wüstefeld et al. [2009] database, as of September 2014. Individual studies include the following: Abt et al. [2010], Assumpção et al. [2006, 2011], Barruol et al. [1997], Barruol and Hoffmann [1999], Bock et al. [1998], Fontaine et al. [2005], Growdon et al. [2009], Heintz et al. [2003], Helffrich et al. [1994], Helffrich et al. [2002], James and Assumpção [1996], Kaneshima and Silver, 1992, Krüger et al. [2002], Masy et al. [2011], Meade et al. [1995], Murdie and Russo [1999], Piñero-Feliciangeli and Kendall, 2008, Polet et al. [2000], Rosa et al. [2012], Russo and Silver [1994], Russo et al. [1996], Silver and Chan [1991], and Vinnik et al. [1992].

distribution of back azimuths with good splitting is limited primarily to the southwest, but observations from the northwest display consistent splitting parameters (see Figure S3). This limitation restricts the analysis to assume a single layer of anisotropy, realizing that averaging properties of SKS splitting are complex [e.g., Becker et al., 2012].

Table 1. Compilation of Average Splitting Parameters at Station With at Least One Good Observation^a

Station Name	Longitude	Latitude	Mean Fast Axis (Degrees Azimuth) (RC)	Mean Delay Time (s) (RC)	Mean Fast Axis (Degrees Azimuth) (SC)	Mean Delay Time (s) (SC)	Mean Fast Axis (Degrees Azimuth) (EV)	Mean Delay Time (s) (EV)
BRR	-73.7	7.1	22	0.55	354	0.7	42	0.35
CHI	-73.7	4.6	17	1.18	2	1.41	12	1.01
ROSC	-74.3	4.8	10	1.45	350	1.6	0	1.5
ZAR	-74.9	7.5	306	1.08	307	1.24	317	1.47
PRA	-74.9	3.7	359	1.17	12	1.24	351	1.25
SJC	-75.2	9.9	314	0.48	272	1.7	330	0.56
RREF	-75.3	4.9	287	1.71	274	2.23	278	1.57
GUY	-75.4	5.2	77	1.05	84	0.46	79	0.39
ANIL	-75.4	4.5	277	0.75	72	1.3	72	1.3
HEL	-75.5	6.2	312	1.22	307	1.18	317	1.35
FLO2	-75.7	1.6	290	0.71	285	0.76	274	0.29
PCON	-76.4	2.3	292	0.71	83	1.27	295	0.41
SOTA	-76.6	2.1	298	1.4	296	1.3	292	1.2
GCUF	-77.3	1.2	285	0.56	287	0.78	273	0.58
OTAV	-78.5	0.2	287	0.67	322	1.24	272	0.57
TUM	-78.7	1.8	280	0.68	295	0.8	83	0.4
MAP	-81.6	4	294	1.96	297	2.04	291	2.03
MARA	-76	2.8	289	0.57	274	0.73	301	0.55

^aAll three methods used in SplitLab are presented, but the text focuses on the rotation correlation (RC) method for interpretation. Values reported do not represent significant figures.

3. Discussion

The observation of consistently trench perpendicular anisotropy along the arc of the Cauca segment fits the standard model of corner flow [McKenzie, 1979] with entrained slab mantle currents. This is consistent with A-type LPO development and simple fluid dynamics, but atypical of most subduction zones (e.g., Figures 1 and 2). The trench-perpendicular trend continues northward, through the suggested Caldas Tear, and into the coastal plains of northern Colombia. However, above the shallow seismicity of the Bucaramanga segment, station BRR indicates an apparent fast orientation of anisotropy parallel to the trend of seismicity. Stations south of the Bucaramanga segment, in the back arc of the Cauca segment, show similar anisotropy to BRR with an orientation mostly north-south.

Due to the consistency across multiple stations and events, the strong spatial variations in fast axes appear to be real. Such a ~90° rotation in anisotropy over distances of ~100 km is uncommon but seen, for example, in the Japan subduction setting [e.g., Long and van der Hilst, 2005]. This indicates that the depth that causes the change of anisotropy occurs is fairly shallow because the three-dimensional Fresnel zones of the utilized SKS paths have little overlap shallower than ~250–300 km depth. This leads us to consider lithospheric signatures, fossil anisotropy in the subducting plate, large-scale asthenospheric flow, and second-order slab-related flow as possible explanations for the observed patterns in splitting.

3.1. Lithospheric and Other Fossil Anisotropy

SKS splitting is expected to be mainly sensitive to asthenospheric flow in the uppermost mantle as this region may be the most susceptible to the coherent development of anisotropic fabric in A-type olivine [e.g., Long and Becker, 2010]. This assumption will be incorrect if there is strong fossil anisotropy within the

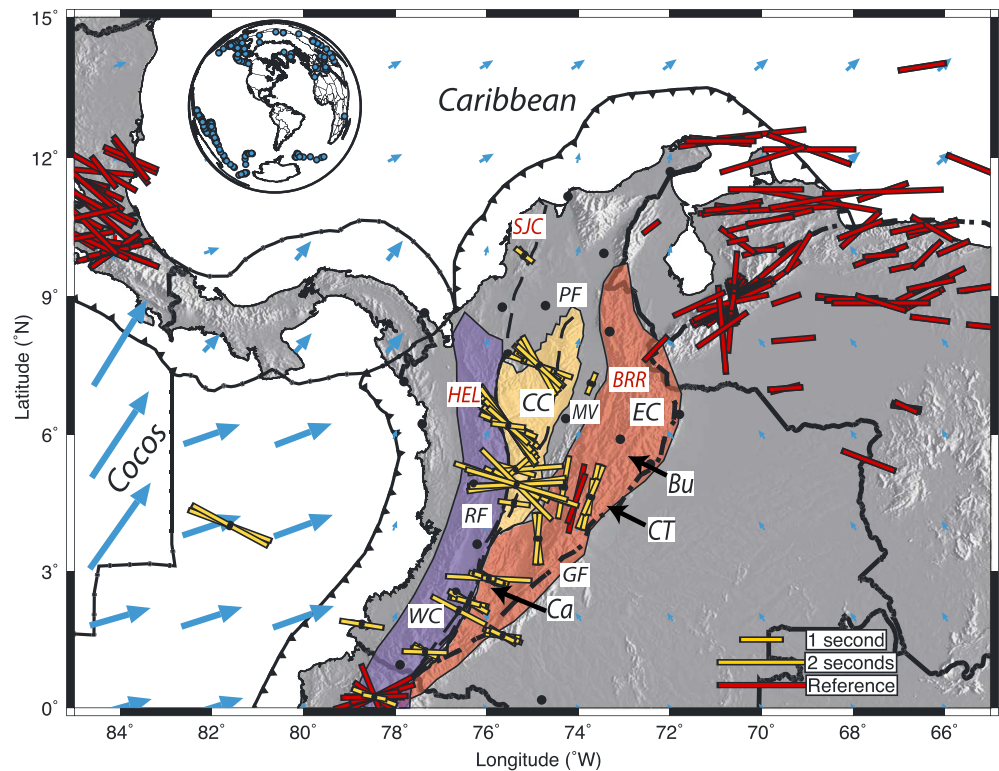


Figure 2. Map of good splitting measurements obtained here and in the references of Figure 1. Black circles represent available stations; large circles without yellow bars indicate no good splitting was observed. Plate boundaries from Bird [2003] plotted in black lines. Earthquakes used as SKS sources for the study are shown in the global inset in the upper left as blue circles. Background topography is from ETOPO1 from NOAA (<http://www.ngdc.noaa.gov/mgg/global/global.html>). Abbreviations: CC (yellow field), Central Cordillera; EC (red field), Eastern Cordillera; GF, Guaicaramo Fault; MV, Magdalena Valley; PF, Palestina Fault; RF, Romeral Fault; WC (blue field), Western Cordillera; Bu, Bucaramanga segment; Ca, Cauca segment; CT, Caldas Tear. Seismic recording stations discussed in the text labeled with red text (BRR, HEL, and SJ). The bar at BRR is immediately west of the label, HEL is east of the label, and SJ is south of the label.

lithosphere or slab, or if there is deep mantle anisotropy. We can address this issue by comparing local and teleseismic observations. Shih *et al.* [1991] report primarily north-south oriented splitting in the Bucaramanga segment from local events recorded on a 16 day temporary network. Splitting reached a maximum of 0.42 s delay for their longest available raypaths from the 160 km deep Bucaramanga Nest [Schneider *et al.*, 1987] and was observed to have an average fast axis of $\sim N5^{\circ}E$. While we only have one high-quality observation above the slab at station BRR, the orientation and delay ($N22^{\circ}E$ and 0.55 s) are broadly consistent with the local splits. This indicates that much of the observed anisotropy may be due to azimuthal anisotropy in the mantle wedge, with some contribution from the slab uppermost mantle. However, it is possible that some of the rotation from trench-perpendicular fast axes to a more north-south aligned orientation (Figures 2 and 3) is caused, or at least affected, by lithospheric-scale shear zones or frozen-in anisotropy in the lithosphere. Lithospheric deformation zones include the north-south grain of sutures throughout much of the region such as the Romeral, Palestina, and Guaicaramo Faults (Figure 2), and the larger-scale compression and assembly of tectonic units during the docking of the Baudo-Panama island arc since ~ 20 Ma.

Another kind of frozen-in anisotropy with orthorhombic character may exist in the asthenosphere underneath oceanic plates, perhaps due to fractionation processes at the spreading center [Song and Kawakatsu, 2012]. This mechanism can account for trench-perpendicular anisotropy for shallowly dipping slabs, and Song and Kawakatsu [2013] were able to match much of the complex splitting observed in southeast Alaska accounting for the variability of the slab dip. The Cauca segment has a dip of $\sim 40^{\circ}$ [e.g., Taboada *et al.*, 2000; Vargas and Mann, 2013], and the Bucaramanga segment is argued to vary in dip from $\sim 20^{\circ}$ to $\sim 50^{\circ}$ depending on its distance from the trench and the Caldas Tear [e.g., Vargas and Mann, 2013]. These dips appear too steep to invoke slab frozen-in anisotropy as an explanation for the trench-perpendicular anisotropy.

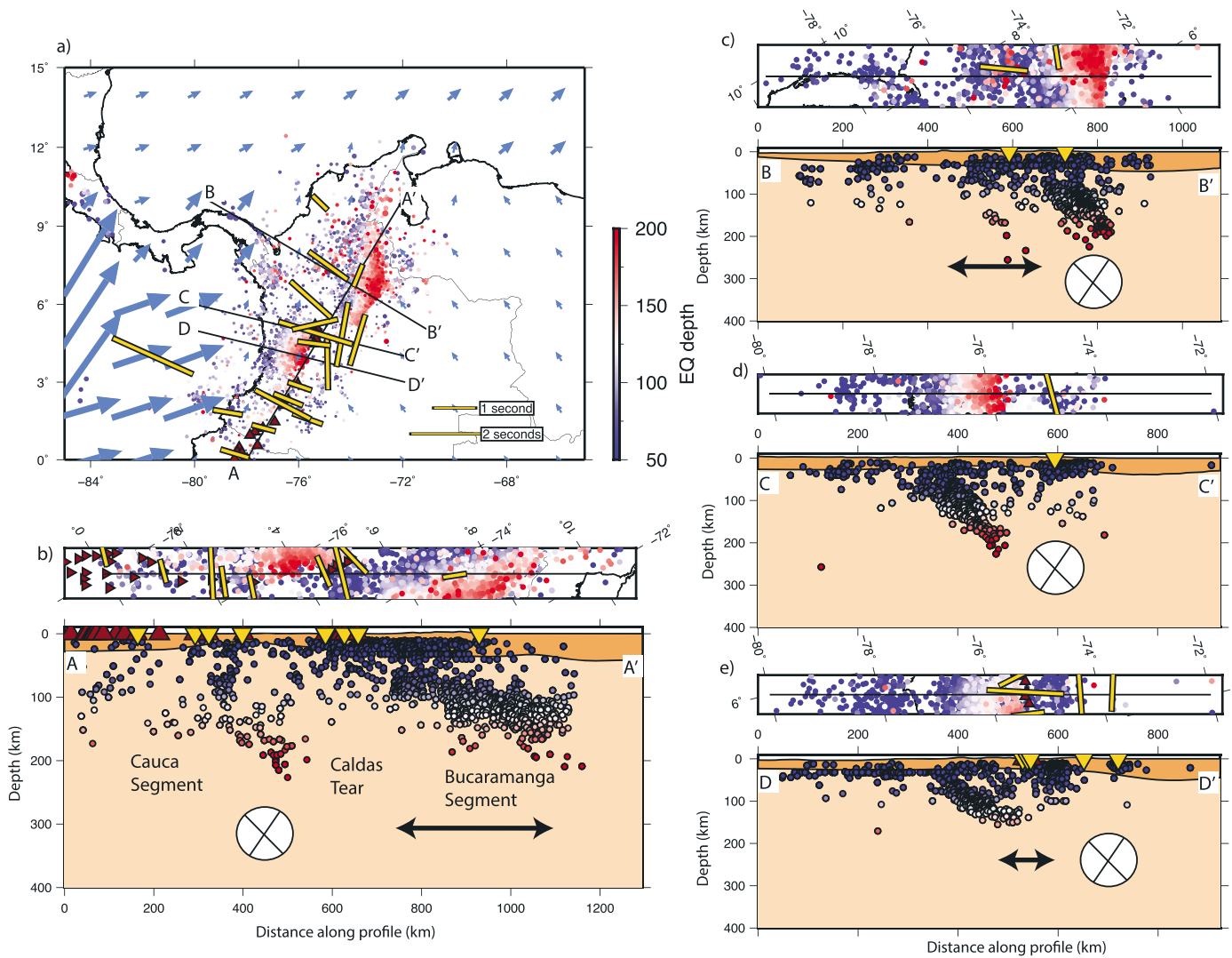


Figure 3. Comparisons between observed splitting and seismically inferred slab structure. (a) Location of profiles in Figures 3b–3e, colored circles with earthquake depth, observed mean splitting, and no-net rotation plate motion vectors plotted. (b–e) Top: oblique Mercator view of seismicity, splitting in oblique projection, and volcanoes (red triangles) near the profiles; bottom: crustal thickness from CRUST1 [Laske et al., 2012] in the darker tan, seismicity within 0.2° of the profile from the RSNC catalog, double-headed arrows indicating anisotropy and inferred mantle flow in the direction of the profile, and circles with crosses indicating anisotropy flow perpendicular to the profile. Red triangles denote volcanoes within 0.5° of the profile and inverted yellow triangles indicate stations within 0.5° of the profile.

3.2. Asthenospheric Anisotropy Other Than Corner Flow

We tested the match of the suite of the global mantle flow models from Miller and Becker [2012], which were scored by these authors against their predictions based on LPO anisotropy as compared to splitting observations east of our study region, mainly in Venezuela. When anisotropy is computed for the stations in our study region, Miller and Becker's best fit model for Venezuela SKS also leads to the best average orientational misfit for our new SKS measurements in Colombia, at ~28° misfit. However, this large-scale flow model fails to capture the observed small-scale variations, as could be expected since it does not include smaller-scale slab anomalies underneath Colombia.

Considering mesoscale slab-induced flow effects to explain the rotation in fast axes, a comparable swing in subduction zone anisotropy has been observed around the southern edge of the Gorda segment of the Juan de Fuca Plate [Özalaybey and Savage, 1995; Zandt and Humphreys, 2008; Eakin et al., 2010; Liu et al., 2012]. There, the signal has been argued to represent either partially frozen-in anisotropy from the removal of the slab [Özalaybey and Savage, 1995] or large-scale toroidal flow [Zandt and Humphreys, 2008]. However, the scale of such toroidal flow appears too large compared to our observations, making it unlikely that toroidal

flow can fully explain the observations, and the lack of a slab window in the region invalidates the hypothesis of partially frozen-in anisotropy from slab removal.

To elucidate possible smaller-scale variations further, Figure 3 presents cross-sectional views of the seismicity in the region (from RSNC) along with our splitting measurements. Profile A-A' (Figure 3b) indicates that three stations at the northern end of the Cauca segment, collocated with Quaternary volcanoes, exhibit trench-perpendicular anisotropy where a lack of intermediate depth earthquakes indicates the Caldas Tear. Stations south of the Caldas Tear also show trench-perpendicular anisotropy, while the station to the north of the tear records a fast axis parallel to the trench. Profile B-B' (Figure 3c) crosses the Bucaramanga segment and displays a pattern where the fore arc exhibits trench normal anisotropy and the station above the slab has a fast axis parallel to the inferred strike of the slab. Profiles C-C' and D-D' (Figures 3d and 3e) cross the Cauca segment and show trench-perpendicular splitting in the northern segment near the Caldas Tear, but trench-parallel splitting in the back arc. The trench-perpendicular anisotropy of the Cauca segment makes this one of the few regions that exhibits this style of anisotropy [Long and Silver, 2008]. The tank experiments of *Buttles and Olson* [1998] and *Druken et al.* [2011] show that a slab undergoing rollback can develop a trench normal mantle flow field from the arc through the back arc. However, the northern South America trenches are only inferred to roll back in some hot spot reference frames and not in the no-net rotation frame [e.g., *Becker and Faccenna*, 2009], and this would not explain variations on a continental scale (Figure 1). Furthermore, the flow field generated by this mechanism should align the back-arc stations in the Eastern Cordillera to be trench normal. Therefore, if rollback-induced mantle flow is occurring, it appears strongly modified by secondary scales of mantle convection or strain in the back arc developed with formation of the north Andean sutures.

An alternative explanation is mantle flow through a tear fault or under a short slab which may lead to trench normal anisotropy [e.g., *Eakin et al.*, 2010]. This seems plausible due to the Caldas Tear, which may allow lateral flow through a slab gap, and seismicity limited to shallower than ~200 km depth in the region of rotation, suggesting the slab does not extend significantly into the asthenosphere. However, the actual location of the slab in this region is unclear. South of ~3°N, the seismicity is poorly resolved in the RSNC catalog, making it difficult to determine a Wadati-Benioff zone in southern Colombia and Northern Ecuador. Further complicating matters, in the Central Cordillera, the Quaternary volcanoes appear to align with the 150 km depth contour of seismicity (see Figure 3d), which may be significantly deeper than the global average of 100 km depth [e.g., *England and Katz*, 2010].

It thus appears that our measurements do not fit well with any single one of the previously suggested models of subduction zone anisotropy [e.g., *Long*, 2013]. Instead, a combination of relatively simple, trench-perpendicular flow alignment in a corner flow subduction scenario with either a lithospheric, or slab gap-induced, anomaly, and/or strong variations of azimuthal anisotropy along the SKS path may have to be invoked. Continued broadband seismic monitoring by the RSNC will provide future opportunities to revisit these questions and more thoroughly sample the anisotropy in the region.

Acknowledgments

The seismic data for this study came from the National Seismological Network of Colombia (Red Sismológica Nacional de Colombia) operated by the Colombian Geological Survey (*Servicio Geológico Colombiano*), and the SplitLab software was provided by Andreas Wüstefeld at <http://splitting.gm.univ-montp2.fr/>. We much appreciate a helpful review of an earlier version of this manuscript by Martha Savage and discussions with Meghan S. Miller, Leland O'Driscoll, and Daoyun Sun. R.W.P.'s funding is provided by NSF-EAR Postdoctoral Fellowship grant 1249776, and T.W.B. was supported by NSF-EAR 1215720. Figures were made with the Generic Mapping Tools [Wessel and Smith, 1998].

The Editor thanks Martha Savage for assistance in evaluating this paper.

4. Conclusions

The Cauca and Bucaramanga slab segments of Colombia are reflected in a complex pattern of seismic anisotropy in western Colombia. Fast axes suggest largely trench-perpendicular shearing throughout much of the region, but with rotation to a roughly trench-parallel signal in the back arc over distances of ~100 km. Such a signal is atypical globally but generally fits with the classical model of corner flow alignment in subduction zones. The rapid rotation to trench-parallel fast axes in the Cauca back arc and along the Bucaramanga segment could be related to a lithospheric signature, or asthenospheric flow through the suggested Caldas Tear, which would imply mechanical separation between the Cauca and Bucaramanga segments. Our findings speak to the relationship between slab dynamics and tectonics in Colombia but are also a challenge to both our understanding of the link between mantle flow and anisotropy, and the general interpretation of subduction zone anisotropy.

References

- Abt, D. L., K. M. Fischer, G. A. Abers, M. Protti, V. González, and W. Strauch (2010), Constraints on upper mantle anisotropy surrounding the Cocos slab from SK(K)S splitting, *J. Geophys. Res.*, *115*, B06316, doi:10.1029/2009JB006710.
- Argus, D. F., R. G. Gordon, and C. DeMets (2011), Geologically current motion of 56 plates relative to the no-net-rotation reference frame, *Geochem. Geophys. Geosyst.*, *12*, Q11001, doi:10.1029/2011GC003751.

- Assumpção, M., M. Heintz, A. Vauchez, and M. E. Silva (2006), Upper mantle anisotropy in SE and Central Brazil from SKS splitting: Evidence of asthenospheric flow around a cratonic keel, *Earth Planet. Sci. Lett.*, *250*(1), 224–240, doi:10.1016/j.epsl.2006.07.038.
- Assumpção, M., M. Guarido, S. van der Lee, and J. C. Dourado (2011), Upper-mantle seismic anisotropy from SKS splitting in the South American stable platform: A test of asthenospheric flow models beneath the lithosphere, *Lithosphere*, *3*(2), 173–180, doi:10.1130/L99.1.
- Barruol, G., and R. Hoffmann (1999), Upper mantle anisotropy beneath the Geoscope stations, *J. Geophys. Res.*, *104*(B5), 10,757–10,773, doi:10.1029/1999JB900033.
- Barruol, G., G. Helffrich, and A. Vauchez (1997), Shear wave splitting around the northern Atlantic: Frozen Pangaeian lithospheric anisotropy?, *Tectonophysics*, *279*(1), 135–148, doi:10.1016/S0040-1951(97)00126-1.
- Becker, T. W., and C. Faccenna (2009), A review of the role of subduction dynamics for regional and global plate motions, *Subduction Zone Geodyn.*, 3–34, doi:10.1007/978-3-540-87974-9.
- Becker, T. W., S. Lebedev, and M. Long (2012), On the relationship between azimuthal anisotropy from shear wave splitting and surface wave tomography, *J. Geophys. Res.*, *117*, B01306, doi:10.1029/2011JB008705.
- Becker, T. W., C. P. Conrad, A. J. Schaeffer, and S. Lebedev (2014), Origin of azimuthal seismic anisotropy in oceanic plates and mantle, *Earth Planet. Sci. Lett.*, *401*, 236–250, doi:10.1016/j.epsl.2014.06.014.
- Bird, P. (2003), An updated digital model of plate boundaries, *Geochem. Geophys. Geosyst.*, *4*(3), 1027, doi:10.1029/2001GC000252.
- Bock, G., R. Kind, A. Rudloff, and G. Asch (1998), Shear wave anisotropy in the upper mantle beneath the Nazca plate in northern Chile, *J. Geophys. Res.*, *103*(B10), 24,333–24,345, doi:10.1029/98JB01465.
- Bowman, J. R., and M. Ando (1987), Shear-wave splitting in the upper-mantle wedge above the Tonga subduction zone, *Geophys. J. Int.*, *88*(1), 25–41, doi:10.1111/j.1365-246X.1987.tb01367.x.
- Buttles, J., and P. Olson (1998), A laboratory model of subduction zone anisotropy, *Earth Planet. Sci. Lett.*, *164*(1), 245–262, doi:10.1016/S0012-821X(98)00211-8.
- Cortés, M., and J. Angelier (2005), Current states of stress in the northern Andes as indicated by focal mechanisms of earthquakes, *Tectonophysics*, *403*(1), 29–58, doi:10.1016/j.tecto.2005.03.020.
- Druken, K., M. Long, and C. Kincaid (2011), Patterns in seismic anisotropy driven by rollback subduction beneath the High Lava Plains, *Geophys. Res. Lett.*, *38*, L13310, doi:10.1029/2011GL047541.
- Eakin, C. M., M. Obrebski, R. M. Allen, D. C. Boyarko, M. R. Brudzinski, and R. Porritt (2010), Seismic anisotropy beneath Cascadia and the Mendocino triple junction: Interaction of the subducting slab with mantle flow, *Earth Planet. Sci. Lett.*, *297*(3), 627–632, doi:10.1016/j.epsl.2010.07.015.
- England, P. C., and R. F. Katz (2010), Melting above the anhydrous solidus controls the location of volcanic arcs, *Nature*, *467*, 700–704, doi:10.1038/nature09417.
- Faccenna, M., and F. A. Capitanio (2013), Seismic anisotropy around subduction zones: Insights from three-dimensional modeling of upper mantle deformation and SKS splitting calculations, *Geochem. Geophys. Geosyst.*, *14*, 243–262, doi:10.1002/ggge.20055.
- Fontaine, F. R., E. E. Hooft, P. G. Burkett, D. R. Toomey, S. C. Solomon, and P. G. Silver (2005), Shear-wave splitting beneath the Galápagos archipelago, *Geophys. Res. Lett.*, *32*, L21308, doi:10.1029/2005GL024014.
- Growdon, M. A., G. L. Pavlis, F. Niu, F. L. Vernon, and H. Rendon (2009), Constraints on mantle flow at the Caribbean-South American plate boundary inferred from shear wave splitting, *J. Geophys. Res.*, *114*, B02303, doi:10.1029/2008JB005887.
- Gutscher, M., W. Spakman, H. Bijwaard, and E. R. Engdahl (2000), Geodynamics of flat subduction: Seismicity and tomographic constraints from the Andean margin, *Tectonics*, *19*(5), 814–833, doi:10.1029/1999TC001152.
- Hall, C. E., K. M. Fischer, E. Parmentier, and D. K. Blackman (2000), The influence of plate motions on three-dimensional back arc mantle flow and shear wave splitting, *J. Geophys. Res.*, *105*(B12), 28,009–28,033, doi:10.1029/2000JB900297.
- Heintz, M., A. Vauchez, M. Assumpção, G. Barruol, and M. Egidio-Silva (2003), Shear wave splitting in SE Brazil: An effect of active or fossil upper mantle flow, or both?, *Earth Planet. Sci. Lett.*, *211*(1), 79–95, doi:10.1016/S0012-821X(03)00163-8.
- Helffrich, G., P. Silver, and H. Given (1994), Shear-wave splitting variation over short spatial scales on continents, *Geophys. J. Int.*, *119*(2), 561–573, doi:10.1111/j.1365-246X.1994.tb00142.x.
- Helffrich, G., D. A. Wiens, E. Vera, S. Barrientos, P. Shore, S. Robertson, and R. Adaros (2002), A teleseismic shear-wave splitting study to investigate mantle flow around South America and implications for plate-driving forces, *Geophys. J. Int.*, *149*(1), F1–F7, doi:10.1046/j.1365-246X.2002.01636.x.
- James, D. E., and M. Assumpção (1996), Tectonic implications of S-wave anisotropy beneath SE Brazil, *Geophys. J. Int.*, *126*(1), 1–10, doi:10.1111/j.1365-246X.1996.tb05263.x.
- Kaneshima, S., and P. G. Silver (1992), A search for source side mantle anisotropy, *Geophys. Res. Lett.*, *19*(10), 1049–1052, doi:10.1029/92GL00899.
- Karato, S. I., H. Jung, I. Katayama, and P. Skemer (2008), Geodynamic significance of seismic anisotropy of the upper mantle: New insights from laboratory studies, *Ann Rev. Earth Planet. Sci.*, *36*, 59–95, doi:10.1146/annurev.earth.36.031207.124120.
- Kneller, E. A., and P. E. van Keken (2008), Effect of three-dimensional slab geometry on deformation in the mantle wedge: Implications for shear wave anisotropy, *Geochem. Geophys. Geosyst.*, *9*, Q01003, doi:10.1029/2007GC001677.
- Krüger, F., F. Scherbaum, J. Rosa, R. Kind, F. Zetsche, and J. Höhne (2002), Crustal and upper mantle structure in the Amazon region (Brazil) determined with broadband mobile stations, *J. Geophys. Res.*, *107*(B10), 2265, doi:10.1029/2001JB000598.
- Laske, G., G. Masters, Z. Ma, and M. E. Pasyanos (2012), CRUST1.0: An updated global model of Earth's crust, *Geophys. Res. Abs.* *14*, EGU2012-3743-1, EGU General Assembly 2012.
- Li, Z. H., J. F. Di Leo, and N. M. Ribe (2014), Subduction-induced mantle flow, finite strain, and seismic anisotropy: Numerical modeling, *J. Geophys. Res. Solid Earth*, *119*, 5052–5076, doi:10.1002/2014JB010996.
- Liu, K., A. Levander, Y. Zhai, R. W. Porritt, and R. M. Allen (2012), Asthenospheric flow and lithospheric evolution near the Mendocino Triple Junction, *Earth Planet. Sci. Lett.*, *323*, 60–71, doi:10.1016/j.epsl.2012.01.020.
- Long, M. D. (2013), Constraints on subduction geodynamics from seismic anisotropy, *Rev. Geophys.*, *51*, 76–112, doi:10.1002/rog.20008.
- Long, M. D., and T. W. Becker (2010), Mantle dynamics and seismic anisotropy, *Earth Planet. Sci. Lett.*, *297*, 341–354, doi:10.1016/j.epsl.2010.06.036.
- Long, M. D., and P. G. Silver (2008), The subduction zone flow field from seismic anisotropy: A global view, *Science*, *319*(5861), 315–318, doi:10.1126/science.1150809.
- Long, M. D., and R. D. van der Hilst (2005), Upper mantle anisotropy beneath Japan from shear wave splitting, *Phys. Earth Planet. Inter.*, *151*, 206–222, doi:10.1016/j.pepi.2005.03.003.
- Mainprice, D. (2007), Seismic anisotropy of the deep Earth from a mineral and rock physics perspective, *Treatise Geophys.*, *2*, 437–491, doi:10.1016/B978-0-44452748-6.00045-6.
- Masy, J., F. Niu, A. Levander, and M. Schmitz (2011), Mantle flow beneath northwestern Venezuela: Seismic evidence for a deep origin of the Mérida Andes, *Earth Planet. Sci. Lett.*, *305*(3), 396–404, doi:10.1016/j.epsl.2011.03.024.

- McKenzie, D. P. (1979), Finite deformation during fluid flow, *Geophys. J. R. Astron. Soc.*, *58*, 689–715, doi:10.1111/j.1365-246X.1979.tb04803.x.
- Meade, C., P. G. Silver, and S. Kaneshima (1995), Laboratory and seismological observations of lower mantle isotropy, *Geophys. Res. Lett.*, *22*(10), 1293–1296, doi:10.1029/95GL01091.
- Miller, M. S., and T. W. Becker (2012), Mantle flow deflected by interactions between subducted slabs and cratonic keels, *Nat. Geosci.*, *5*(10), 726–730, doi:10.1038/ngeo1553.
- Miller, M. S., A. A. Allam, T. W. Becker, J. F. Di Leo, and J. Wookey (2013), Constraints on the tectonic evolution of the westernmost Mediterranean and northwestern Africa from shear wave splitting analysis, *Earth Planet. Sci. Lett.*, *375*, 234–243, doi:10.1016/j.epsl.2013.05.036.
- Montes, C., G. Bayona, A. Cardona, D. M. Buchs, C. A. Silva, S. Morón, N. Hoyos, D. A. Ramirez, C. A. Jaramillo, and V. Valencia (2012), Arc-continent collision and orocline formation: Closing of the Central American seaway, *J. Geophys. Res.*, *117*, B04105, doi:10.1029/2011JB008958.
- Murdie, R. E., and R. M. Russo (1999), Seismic anisotropy in the region of the Chile margin triple junction, *J. South Am. Earth Sci.*, *12*(3), 261–270, doi:10.1016/S0895-9811(99)00018-8.
- Ojeda, A., and J. Havskov (2001), Crustal structure and local seismicity in Colombia, *J. Seismol.*, *5*(4), 575–593, doi:10.1023/A:1012053206408.
- Ózalaybey, S., and M. K. Savage (1995), Shear-wave splitting beneath western United States in relation to plate tectonics, *J. Geophys. Res.*, *100*(B9), 18,135–18,149, doi:10.1029/95JB00715.
- Pennington, W. D. (1981), Subduction of the eastern Panama Basin and seismotectonics of northwestern South America, *J. Geophys. Res.*, *86*(B11), 10,753–10,770, doi:10.1029/JB086B11p10753.
- Piñero-Feliciangeli, L., and J. Kendall (2008), Sub-slab mantle flow parallel to the Caribbean plate boundaries: Inferences from SKS splitting, *Tectonophysics*, *462*(1), 22–34, doi:10.1016/j.tecto.2008.01.022.
- Polet, J., P. Silver, S. Beck, T. Wallace, G. Zandt, S. Ruppert, R. Kind, and A. Rudloff (2000), Shear wave anisotropy beneath the Andes from the BANJO, SEDA, and PISCO experiments, *J. Geophys. Res.*, *105*(B3), 6287–6304, doi:10.1029/1999JB900326.
- Rosa, J. W. C., J. W. C. Rosa, and R. A. Fuck (2012), Crust and upper mantle structure in central Brazil derived by receiver functions and SKS splitting analysis, *J. South Am. Earth Sci.*, *34*, 33–46, doi:10.1016/j.jsames.2011.09.001.
- Russo, R., and P. Silver (1994), Trench-parallel flow beneath the Nazca plate from seismic anisotropy, *Science*, *263*(5150), 1105–1111, doi:10.1126/science.263.5150.1105.
- Russo, R., P. Silver, M. Franke, W. Ambeh, and D. James (1996), Shear-wave splitting in northeast Venezuela, Trinidad, and the eastern Caribbean, *Phys. Earth Planet. Inter.*, *95*(3), 251–275, doi:10.1016/0031-9201(95)03128-6.
- Schneider, J. F., W. D. Pennington, and R. P. Meyer (1987), Microseismicity and focal mechanisms of the intermediate-depth Bucaramanga Nest, Colombia, *J. Geophys. Res.*, *92*(B13), 13,913–13,926, doi:10.1029/JB092iB13p13913.
- Shih, X. R., J. F. Schneider, and R. P. Meyer (1991), Polarities of P and S waves, and shear wave splitting observed from the Bucaramanga Nest, Colombia, *J. Geophys. Res.*, *96*(B7), 12,069–12,082, doi:10.1029/91JB01201.
- Silver, P. G. (1996), Seismic anisotropy beneath the continents: Probing the depths of geology, *Ann. Rev. Earth Planet. Sci.*, *24*, 385–432, doi:10.1146/annurev.earth.24.1.385.
- Silver, P. G., and W. W. Chan (1991), Shear wave splitting and subcontinental mantle deformation, *J. Geophys. Res.*, *96*(B10), 16,429–16,454, doi:10.1029/91JB00899.
- Song, T.-R. A., and H. Kawakatsu (2012), Subduction of oceanic asthenosphere: Evidence from sub-slab seismic anisotropy, *Geophys. Res. Lett.*, *39*, L17301, doi:10.1029/2012GL052639.
- Song, T.-R. A., and H. Kawakatsu (2013), Subduction of oceanic asthenosphere: A critical appraisal in central Alaska, *Earth Planet. Sci. Lett.*, *36*, 82–94, doi:10.1016/j.epsl.2013.02.010.
- Taboada, A., L. A. Rivera, A. Fuenzalida, A. Cisternas, H. Philip, H. Bijwaard, J. Olaya, and C. Rivera (2000), Geodynamics of the northern Andes: Subductions and intracontinental deformation (Colombia), *Tectonics*, *19*(5), 787–813, doi:10.1029/2000TC900004.
- van der Hilst, R., and P. Mann (1994), Tectonic implications of tomographic images of subducted lithosphere beneath northwestern South America, *Geology*, *22*(5), 451–454, doi:10.1130/0091-7613(1994)022<0451:TLOTIO>2.3.co;2.
- Vargas, C. A., and P. Mann (2013), Tearing and breaking off of subducted slabs as the result of collision of the Panama Arc-Indenter with northwestern South America, *Bull. Seismol. Soc. Am.*, *103*(3), 2025–2046, doi:10.1785/0120120328.
- Vinnik, L., L. Makeyeva, A. Milev, and A. Y. Usenko (1992), Global patterns of azimuthal anisotropy and deformations in the continental mantle, *Geophys. J. Int.*, *111*(3), 433–447, doi:10.1111/j.1365-246X.1992.tb02102.x.
- Wessel, P., and W. H. F. Smith (1998), New, improved version of the Generic Mapping Tools released, *Eos Trans. AGU*, *79*, 579, doi:10.1029/98EO00426.
- Wüstefeld, A., G. Bokelmann, C. Zaroli, and G. Barruol (2008), SplitLab: A shear-wave splitting environment in Matlab, *C. R. Geosci.*, *34*(5), 515–528, doi:10.1016/j.cageo.2007.08.002.
- Wüstefeld, A., G. Bokelmann, G. Barruol, and J. Montagner (2009), Identifying global seismic anisotropy patterns by correlating shear-wave splitting and surface-wave data, *Phys. Earth Planet. Inter.*, *176*(3), 198–212, doi:10.1016/j.pepi.2009.05.006.
- Yarce, J., G. Monslave, T. W. Becker, A. Cardona, E. Poveda, D. Alvira, and O. Ordoñez-Carmona (2014), Seismological observations in northwestern South America: Evidence for two subduction segments, contrasting crustal thicknesses and upper mantle flow, *Tectonophysics*, *637*, 57–67, doi:10.1016/j.tecto.2014.09.006.
- Zandt, G., and E. Humphreys (2008), Toroidal mantle flow through the western US slab window, *Geology*, *36*(4), 295–298, doi:10.1130/G24611A.1.